JOURNAL OF GEOPHYSICAL RESEARCH, VOL. 91, NO. B9, PAGES 9183-9192, AUGUST 10, 1986

A GLOBAL POSITIONING SYSTEM BASELINE DETERMINATION INCLUDING BIAS FIXING AND WATER VAPOR RADIOMETER CORRECTIONS

Randolph H. Ware and Christian Rocken

Cooperative Institute for Research in Environmental Sciences,
University of Colorado, Boulder, Colorado

Kenneth J. Hurst

Lamont-Doherty Geological Observatory, Palisades, New York

Abstract. We report a Global Positioning System (GPS) baseline determination which includes bias fixing (carrier phase ambiguity solutions) and tropospheric corrections based on simultaneous water vapor radiometer (WVR) observations. Measurements were obtained using single-wavelength codeless GPS receivers and dual-wavelength WVRs at each end of a 22-km baseline near Boulder, Colorado, during three evenings in July 1983. Local thunderstorm activity prevailed during these observations. The WVRs were pointed toward each satellite sequentially at 15-min intervals during GPS data acquisition. Radio path delay corrections as large as 10 cm were estimated from the WVR observations. Baseline vectors were determined using tropospheric corrections based on WVR and surface meteorological (met) measurements and by resolving phase ambiguities (bias fixing). A repeat measurement of the same baseline was performed without WVRs during clear weather conditions in September 1984. If WVR corrections were not applied, we found that time varying corrections based on surface met measurements improved baseline length repeatability by a factor of 2, compared to corrections based on default surface met values. Applying WVR corrections in bias-fixed baseline solutions, we found a 4-cm decrease in relative height and a corresponding factor of 3 improvement in the repeatability (to 0.6 ppm). The WVR corrections also enhanced our ability to resolve phase ambiguities. Bias-free solutions, with the WVR correction, showed essentially the same 4-cm decrease in the vertical component (with the repeatability improved to 1 ppm). Baseline solutions using simulated data that include only the WVR correction confirm this decrease in the vertical. These results suggest that during disturbed weather conditions WVR (and surface P and T) measurements may be useful in achieving reliable bias fixing as well as optimum vertical accuracy.

Introduction

It has been predicted that corrections based on water vapor radiometer (WVR) observations will be required to routinely attain relative positioning accuracy on the order of a centimeter over 100-km baselines using the NAVSTAR Global Positioning System (GPS) [Bossler et al., 1980; Bender and Larden, 1985]. Such corrections account for the refractive phase delay of satellite radio signals by tropospheric water vapor. We expect that improved orbit determinations, ionospheric corrections based on dual-frequency observations, and carrier phase ambiguity resolution will also be required to attain maximum accuracy for GPS baseline measurements, particularly in the case of baselines longer than about 50 km.

Phase ambiguity resolution is the determination of the integer number of wavelengths to each satellite, also known as "bias-fixing." If the phase ambiguities are not fixed to integers, a baseline solution is termed "bias free." Phase ambiguity resolution is not obtained directly from the carrier phase measurements observed by GPS receivers but must be determined independently. Successful bias fixing generally improves the accuracy of the baseline determination by a factor of 2 or more. Although bias-fixed baseline determinations have been previously reported [Bock et al., 1985; Strange, 1985], their solutions did not include WVR corrections.

We present single frequency baseline determinations for bias-free and bias-fixed cases and compare the repeatabilities using wet-troposphere corrections based on WVR observations or surface meteorological data. We find that WVR corrections significantly change the vertical baseline component, and compared to surface met corrections, they improve the baseline repeatability and allow more reliable bias fixing.

Experimental Technique

Two single-frequency Macrometer^{TM} GPS receivers operated by the National Geodetic Survey [Goad et al., 1984; Counselman et al., 1982] and two dual-frequency water vapor radiometers developed by the National Oceanic and Atmospheric Administration (NOAA) were operated simultaneously at both ends of a 22-km baseline located near Boulder, Colorado. Survey marks were placed at both sites in June 1983 by the National Geodetic Survey (NGS). The baseline is oriented nearly east-west and is located on the high plains just to the east of the Rocky Mountain cordillera.

Paper number 5B5688.
0148-0227/86/0005B-5688$05.00

Five NAVSTAR satellites were observed on three consecutive evenings July 17-19, 1983, from 1650 to 1930 Rocky Mountain Daylight Time (RMDT). WVR observations were taken simultaneously. The receivers observed only the L1 frequency at 1575.42 GHz (19.03-cm wavelength). Surface meteorological (met) measurements, including barometric pressure (P), dry bulb temperature (T), and wet bulb temperature, were recorded at the start and finish times. On September 6, 1984, the same baseline was measured again observing six satellites (1235 to 1529 RMDT). For this observation, surface met measurements were recorded at the start, midpoint, and finish times, but WVR data were not recorded. Local weather was clear and dry during the 1984 observation.

In the surface met instrument package, a battery-powered fan moved air around the wet bulb. Relative humidity (RH) was determined from wet and dry bulb temperatures using standard tables [Hodgman et al., 1961]. The apparatus was placed under the tripod, over the survey mark, on top of the ground. No attempt was made to shield the thermometers from sunlight. The thermometers were also subject to influence by the humidity and temperature of the local ground surface, which was exposed to precipitation and sunlight. Taking these factors into account, the NGS estimates that the surface measurements were accurate to P,± 1 mbar, T, ± 0.5 ° C, and RH, ± 10%.

The NOAA WVRs [Hogg et al., 1983] operate at 20.6 GHz (sensitive to water vapor) and 31.6 GHz (sensitive to liquid water). Water vapor and liquid were estimated independently by solving two simultaneous equations using statistical retrieval methods. The algorithm corrects the water vapor measurement for the presence of liquid ranging up to 1 g/m^3 in nonprecipitating clouds and also corrects for the sensitivity of both channels to atmospheric oxygen. The radiometer antenna, fully steerable in azimuth and elevation, is designed to produce a 2.5 ° angular beamwidth at both frequencies. WVRs were calibrated using elevation scans (tipping curves) on stable, cloudless days. For use in pointing the WVRs, preliminary ephemeris data were provided for each 3-min epoch by the NGS. For baseline analysis we used precise ephemeris data with accuracies of about 30 m, provided by the Naval Surface Weapons Center. The WVRs were located within 50 m of each GPS receiver, and they were pointed toward each satellite every 15 min. This allowed 2 min to change the pointing and 1 min for observation toward each of the five satellites. By this method the line-of-sight integrated water vapor to each satellite was measured every 15 min.

Data Processing

WVR data were processed in real time using a data acquisition program that computes the integrated water vapor and liquid at 1-s intervals. These quantities were averaged for 10 s and stored for later conversion to excess path corrections [Hogg et al., 1981] or phase delay. Liquid-bearing clouds were present near both measurement sites during the 1983 observation. Since the accuracy of the water vapor determination is degraded when several centimeters or more of liquid water is observed, water vapor levels were estimated from adjacent reliable data points in such cases.

Baseline coordinates were calculated using software developed by the NGS [Remondi, 1984] and modified by C. Rocken to allow WVR corrections, automatic fixing of phase ambiguities, and corrections for earth rotation. The coordinates for the two sites in the 1972 World Geodetic System (WGS72) datum are 40 ° 00′43.035" latitude, 105 ° 15′04.967" longitude, 1571.02 m height (in the city of Boulder, labeled "Ware" on the survey mark), and 39 ° 59′36.579" latitude, 104 ° 59′38.515" longitude, 1559.47 m height (near the town of Erie, labeled "Slater" on the survey mark). The Boulder coordinates were held fixed and the Erie coordinates were determined.

The calculation was carried out in two steps. The first step subtracts the phases recorded at stations A and B for each satellite at each epoch to form the single difference

$$\Delta\Phi = \Phi_A - \Phi_B \tag{1}$$

where Φ_A and Φ_B contain phase delays from the ionosphere (Φ_{Aion}; Φ_{Bion}) and the dry (Φ_{Adry}; Φ_{Bdry}) and wet (Φ_{Awet}; Φ_{Bwet}) components of the troposphere. The single difference can therefore be expressed as

$$\Delta\Phi = (\Phi_{Avac} + \Phi_{Adry} + \Phi_{Awet} + \Phi_{Aion}) - (\Phi_{Bvac} + \Phi_{Bdry} + \Phi_{Bwet} + \Phi_{Bion}) \tag{2}$$

where Φ_{Avac} and Φ_{Bvac} are the phases at stations A and B for a GPS signal traveling through a vacuum. If the wet and the dry corrections are known, and the ionospheric error is neglected, which is reasonable for short baselines where the signal traverses nearly the same ionosphere for both sites, the corrected single differences can be computed from

$$\Delta\Phi_{corr} = (\Phi_{Avac} - \Phi_{Bvac}) = \Delta\Phi + (\Phi_{Bwet} - \Phi_{Awet}) + (\Phi_{Bdry} - \Phi_{Adry}) \tag{3}$$

The second step of the calculation determines the receiver coordinates from a least squares fit of the corrected differences, using satellite ephemerides and considering the geometry of the receivers and satellites.

The tropospheric terms Φ_{dry} and Φ_{wet} in equation (3) were calculated using two different methods. Both methods used the Saastamoinen/Hopfield atmospheric model [Hopfield, 1969; Saastamoinen, 1972a,b,c; Goad, 1974] to calculate Φ_{dry} from surface pressure (P) and temperature (T) measurements. However, Φ_{wet} was

TABLE 1. Surface Meteorological Measurements From the Boulder and Erie Sites

Date	Boulder/Erie			
	Local Time	P, mbar	T, °C	RH, %
July 17, 1983	1624/1630	836.8/837.5	27.5/29.0	54/38
(198)	1930/1927	837.9/838.2	26.0/23.0	39/55
July 18, 1983	1625/1647	843.3/841.9	27.5/24.5	37/43
(199)	1930/1927	843.3/843.6	26.8/25.5	47/36
July 19, 1983	1624/1630	841.6/841.2	28.5/30.0	32/39
(200)	1930/1927	842.3/841.9	26.0/25.5	44/40
Sept. 6, 1984	1245/1227	830/832	33.3/31.9	7/11
(250)	1403/1400	828/830	32.2/33.4	13/11
	1517/1520	827/829	32.8/33.6	10/11

calculated either from surface relative humidity (RH) measurements for one method or from WVR data for the other. The surface met measurements for each receiver site are listed in Table 1. Because of inaccuracies associated with the surface met measurements, which are described in the experimental technique section, default values (P = 840 mbar, T = 25 °C, RH = 50%) were also used in the model in some cases.

For corrections based on WVR data the tropospheric phase delay

$$\Phi_{wet} = V * \frac{6.5}{\lambda_{eff}} \quad (4)$$

resulting from water vapor along the line-of-sight to each satellite was calculated. The factor "6.5" converts the WVR-measured integrated water vapor V (cm) to excess path delay [Hogg et al., 1981]. For the type of codeless receiver data used in this experiment the effective wavelength, λ_{eff}, is half of the 19.0-cm carrier wavelength.

The GPS data were divided into three different groups:

1. T_{sm}, total receiver data set. This set uses surface P, T, and RH data (or default values) to correct for tropospheric path delay.
2. S_{sm}, receiver subset with simultaneous WVR data. This subset uses surface P, T, and RH data (or default values) to correct for tropospheric path delay.
3. S_{wvr}, receiver subset with simultaneous WVR data. This subset uses WVR and surface P and T data (or default values) to correct for tropospheric path delay.

We analyzed each group using a simple algorithm for automatic bias fixing that we added to a modified version of the NGS single difference software. After a bias-free solution was found the program searched for the minimum value of

$$\Delta\lambda_k \ (cycles) = | \epsilon_k | + 3\sigma_k \quad (5)$$

Here ϵ_k is the difference between the number of cycles for satellite k and the closest integer and σ_k is the standard deviation of the least squares fit for that solution as computed from the covariance matrix. The bias with the smallest $\Delta\lambda_k$ was fixed to the nearest integer. This was done for all spacecraft sequentially.

We used the following simple test to determine whether or not the automatic bias-fixing procedure provided reasonable confidence in a given solution. If $\sigma_k < 1/3$ and $\epsilon_k < 1/3$, we considered the bias fixing to be successful, if not, it was considered to be a failure.

Using this simple, automatic bias-fixing procedure we computed baselines for the sets T_{sm}, S_{sm}, and S_{wvr}, with spacecraft 4 as the reference satellite. Here the reference satellite is the one chosen for differencing with each of the other satellites. The reference satellite bias is not fixed to an integer value because it includes the initial relative receiver clock offset. The biases of the other satellites are computed relative to the reference satellite and are therefore independent of receiver clock drift. The initial relative clock offset (receiver clock 1 minus receiver clock 2) was obtained from the NGS field log, assuming linear clock drifts. We handled the initial common clock offset (satellite clock minus average receiver clock) in two ways. In the first case we solved for it, and in the second case we set it equal to zero.

Results

Azimuth and elevation plots of the observed satellites are shown in Figure 1. The entire arcs represent the total GPS data sets, and the asterisks indicate the subset for which WVR data were obtained. Three-minute observation intervals are indicated. The most favorable data, from the standpoint of duration and distribution of satellite arcs, were collected on day 250 in 1984, including six satellites for up to 177 min. However, only surface met data were obtained on day 250. For days 198-200 in 1983, fewer satellites were observed for shorter periods, but WVR and surface met data were obtained. Taken together, these data allow a comparison of GPS baseline repeatabilities with corrections for the wet troposphere based on WVR or surface met data.

Typical examples of the excess path errors resulting from water vapor (wet path delay), measured by

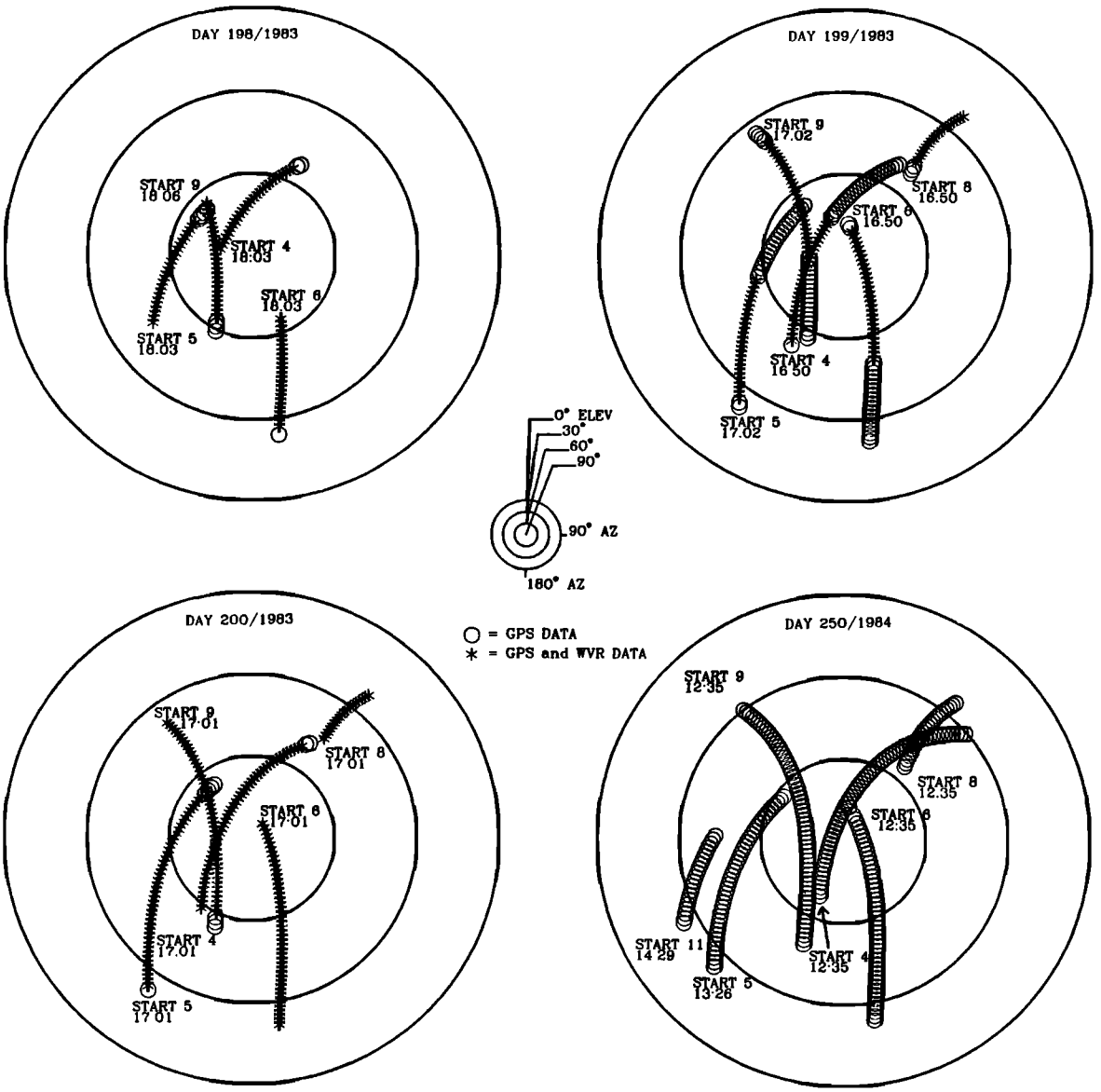

Fig. 1. Azimuth and elevation plots for the observed satellites. Simultaneous GPS and WVR observations are indicated by asterisks, GPS alone by circles. The interval between data points is 3 min. The start times are indicated in Rocky Mountain Daylight Time.

WVRs along the line-of-sight to two of the observed satellites, are shown in Figure 2 for each day of data collection in 1983. Spline fits were used to estimate wet paths during the 15-min intervals between WVR observations toward each satellite. The line-of-sight wet path delay during the observations ranged from 12 to 60 cm. The general sloping curvature seen in Figure 2 is caused by changes in the total amount of observed water vapor with elevation angle as the satellites track across the sky at 30° per hour. The short-term variations or "bumps" are the signatures of local thunderstorms that were present during the three evenings of observations. Similar plots for all of the observed satellites were presented in an earlier paper [Ware et al., 1985] and are not included here.

The wet path difference (Φ_{wet}) for Boulder minus Erie is also shown in Figure 2. This difference, which varies from -6 to +10 cm, represents the phase error resulting from tropospheric water vapor for a particular satellite at a given time during the observations. Similarly, the total tropospheric path delay ($\Phi_{dry} + \Phi_{wet}$) for day 198, is shown in Figure 3. Two correction models are shown in Figure 3 for each satellite. Both models are based on the P and T data listed in Table 1. The lower, sweeping curves use RH values from Table 1, and the curves above use WVR data. The structure seen in the upper curves is attributed to changes in wet path delay as storm clouds are intersected by the line-of-sight from receiver to satellite. On this day the disagreement in path delay for the two models is as large as 4 cm (satellite 6). Similar comparisons on days 199 and 200 showed disagreement as large as 10 cm. Such discrepancies, resulting in part from azimuthal variations in water vapor, cannot be

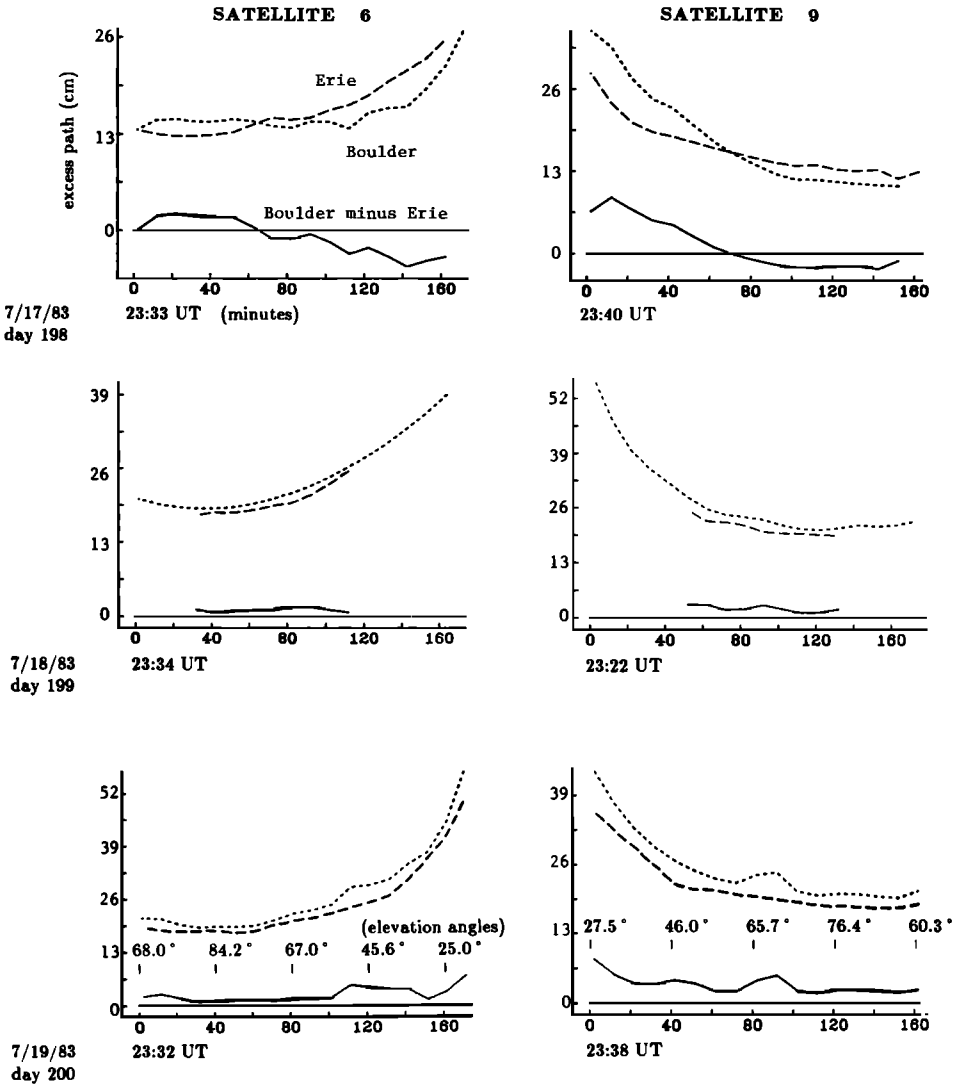

Fig. 2. Wet path delays (Φ_{wet}) estimated from spline fits of WVR measurements at 15-min intervals along the line-of-sight to two NAVSTAR satellites for each of the three days of observations in July 1983. Wet path delays are indicated for each site and for the difference between the two sites. Zenith angles are marked at 40-minute intervals on Julian day 200. Plots for the other three observed satellites are similar and can be seen in the work by Ware et al. [1985].

corrected using models based on surface met data. They also cannot be corrected by solving for the zenith path delay as an additional parameter in the least squares baseline solution.

Baseline component solutions (Boulder minus Erie) for the data sets T_{sm}, S_{sm}, and S_{wvr} are listed in Table 2 (bias-fixed) and Table 3 (bias-free). Also listed are the average value for each component and the standard deviation, which is a measure of the repeatability. The last column in Table 2 indicates whether or not our criteria (equation 5) for successful bias-fixing were satisfied. For the solutions in Tables 2 and 3, default values for surface pressure and temperature, and either WVR data or default relative humidity values were used for tropospheric correction. Inaccuracies in the surface met data, which were interpolated between measurements 3 hours apart for the 1983 data, led us to obtain solutions using measured as well as default values In any case, the baseline solutions are much more sensitive to relative changes in P, T, and RH values between the two sites, compared to simultaneous changes in these parameters at both sites. Similar solutions using the observed surface met data (Table 1) are listed in Table 4. The results listed in Tables 2 and 3 are plotted in Figures 4 and 5, including baseline length, height, and coordinates X, Y, and Z.

Also shown in Figures 4 and 5 are solutions computed from simulated receiver data. The simulated solutions, indicated as vertical lines, include wet path delays computed from WVR data and exclude other errors. They are useful in predicting the effect of WVR corrections on the baseline components, particularly for the bias-free case. For the bias-fixed case, the simulated results are strongly influenced by the ambiguity

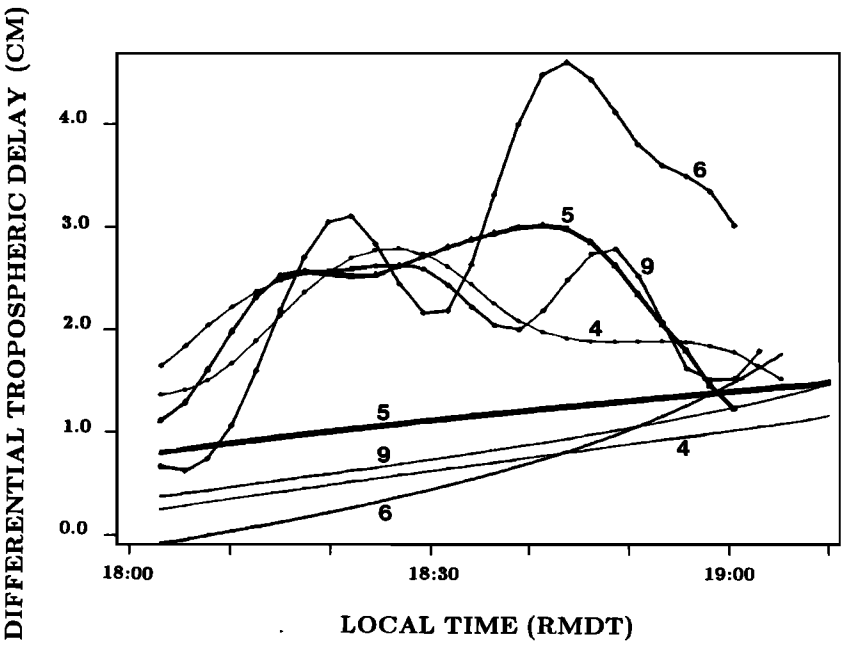

Fig. 3. Total differential tropospheric path delay ($\Phi_{dry} + \Phi_{wet}$) for day 198 computed using two different models. Both models used surface pressure and temperature measurements interpolated from Table 1. The lower, sweeping curves used surface relative humidity measurements and the upper curves used WVR data. All curves are labeled to indicate the satellite number.

resolution, and the wet path delay cannot be separated from this influence. By comparing the vertical lines to the columns (real solutions) immediately to their left, the sum of all errors other than wet path can be estimated. Ionospheric, orbit, multipath, receiver, and clock errors are expected to contribute to this sum.

We also calculated baselines including a common time solution. For the more complete data set on day 250, which was obtained during clear and stable weather conditions compared to the other days, the baseline components agreed to within 2 cm (bias-free) and 0.1 cm (bias-fixed) with solutions where the com-

TABLE 2. Bias-Fixed Baseline Solutions Using Default Surface met (P = 840 mbar, T = 25 ° C, and RH = 50%) and WVR Corrections

Data Set/ Correction	Day/Year	Points	Length 22,075 m + [cm]	Height 11 m + [cm]	X 20,877 m + [cm]	Y −6998 m + [cm]	Z −1577 m + [cm]	Fixing[1]
Total/	198/83	113	89.3	53.7	69.4	−20.0	−95.6	F
default	199/83	224	81.4	61.9	68.6	−12.3	−99.9	S
P,T,RH	200/83	215	81.3	60.2	68.4	−12.8	−97.9	F
	250/84	251	82.8	61.9	70.1	−12.3	−99.4	S
	Average		83.7	59.4	69.1	−14.4	−98.2	
	Standard deviation		3.3	3.4	0.7	3.3	1.7	
Subset/	198/83	103	89.1	52.6	68.9	−20.8	−95.0	F
default	199/83	133	81.2	63.2	68.5	−11.6	−101.1	F[2]
P,T,RH	200/83	201	81.4	60.2	68.5	−12.8	−97.8	F
	Average		83.9	58.7	68.6	−15.1	−98.0	
	Standard deviation		3.7	4.5	0.2	4.1	2.5	
Subset/	198/83	103	84.9	56.3	70.4	−18.3	−97.5	S
WVR,	199/83	133	80.9	53.4	66.3	−18.8	−94.7	S
default P,T	200/83	200	81.9	54.4	67.7	−17.7	−94.7	S
	Average		82.6	54.7	68.1	−18.3	−95.6	
	Standard deviation		1.7	1.2	1.7	0.5	1.3	

[1]success S; failure F.

[2]To obtain this solution, bias values were forced to agree with the WVR-corrected subset on day 199. The automatic bias-fixing solution disagreed by 12 cm in length with the solution listed.

TABLE 3. Bias-Free Baseline Solutions Using Default Surface met (P = 840 mbar, T = 25 °C, and RH = 50%) and WVR Corrections

Data Set/ Correction	Day/Year	Points	Length 22,075 m + [cm]	Height 11 m + [cm]	X 20,877 m + [cm]	Y −6998 m + [cm]	Z −1577 m + [cm]
Total/	198/83	113	87.2	54.3	71.6	−22.0	−98.2
default	199/83	224	86.8	61.7	73.4	−14.8	−100.9
P,T,RH	200/83	215	83.2	59.8	69.8	−14.6	−98.9
	248/84	251	77.2	62.6	64.9	−10.2	−99.6
	Average		83.6	59.6	69.9	−15.4	−99.4
	Standard deviation		4.0	3.2	3.1	4.2	1.0
Subset/	198/83	103	87.7	52.7	71.2	−23.6	−97.6
default	199/83	133	96.0	61.5	82.5	−16.7	−100.0
P,T,RH	200/83	201	84.8	60.3	71.4	−14.6	−99.1
	Average		89.5	58.2	75.0	−18.3	−98.9
	Standard deviation		4.7	3.9	5.3	3.8	1.0
Subset/	198/83	103	79.2	57.7	65.0	−16.3	−99.0
WVR,	199/83	133	79.7	52.6	64.8	−19.3	−94.6
default P,T	200/83	200	79.9	54.2	65.6	−17.8	−95.1
	Average		79.6	54.8	65.1	−17.8	−96.2
	Standard deviation		0.3	2.1	0.3	1.2	2.0

mon time offset was held fixed and assumed to be zero. For the T_{sm} data sets on days 198 and 199, which are observations of more limited duration, the common time solutions disagreed by up to 10 cm. For the subsets S_{sm} and S_{wvr} on days 198 and 199, the common time solutions gave unreasonable results. We attribute this to the short observation times for the subsets on these two days. The unreasonable results encouraged us to present only solutions for which the common time offset was assumed to be zero.

Comments

We find that the differential tropospheric signature is relatively large (up to 10 cm), which we attribute to the local thunderstorm activity that prevailed during the observations. This signature has a significant influence on the vertical baseline component. For the bias-fixed case (Table 2), where default P and T values were used, and either WVR data or default RH values, the vertical component decreases by 4 cm when the WVR correction is applied, and the repeatability improves by

TABLE 4. Bias-Fixed Baseline Solutions Using Measured Surface met (Interpolated From Table 1) and WVR Corrections

Data Set/ Correction	Day/Year	Points	Length 22,075 m + [cm]	Height 11 m + [cm]	X 20,877 m + [cm]	Y −6998 m + [cm]	Z −1577 m + [cm]	Fixing[1]
Total/	198/83	113	84.5	54.6	69.8	−19.4	−96.2	F
surface	199/83	224	81.4	58.7	67.9	−14.6	−97.6	F
P,T,RH	200/83	210	81.4	61.2	68.8	−11.9	−98.3	F
	250/84	253	83.1	62.3	70.4	−12.1	−99.8	S
	Average		82.6	59.7	69.3	−14.5	−98.2	
	Standard deviation		1.3	3.0	1.1	3.0	0.8	
Subset/	198/83	103	84.3	53.3	69.3	−20.3	−95.5	F
surface	199/83	133	81.3	60.4	68.0	−13.7	−99.2	F[2]
P,T,RH	200/83	201	81.4	61.3	68.8	−11.9	−98.2	F
	Average		82.3	58.3	68.7	−15.3	−97.6	
	Standard deviation		1.4	3.6	0.5	3.6	1.6	
Subset/	198/83	103	85.1	55.8	70.5	−18.7	−97.2	S
1WVR,	99/83	133	81.2	52.3	66.4	−19.6	−94.0	F
Surface P,T	200/83	199	82.2	54.3	67.9	−17.9	−94.6	S
	Average		82.8	54.1	68.3	−18.7	−95.3	
	Standard deviation		1.7	1.4	1.7	0.7	1.4	

[1]success S; failure F.

[2]To obtain this solution, bias values were artifically fixed to agree with the WVR-corrected subset on day 199. The automatic bias-fixing solution disagreed by 12 cm in length with the solution listed.

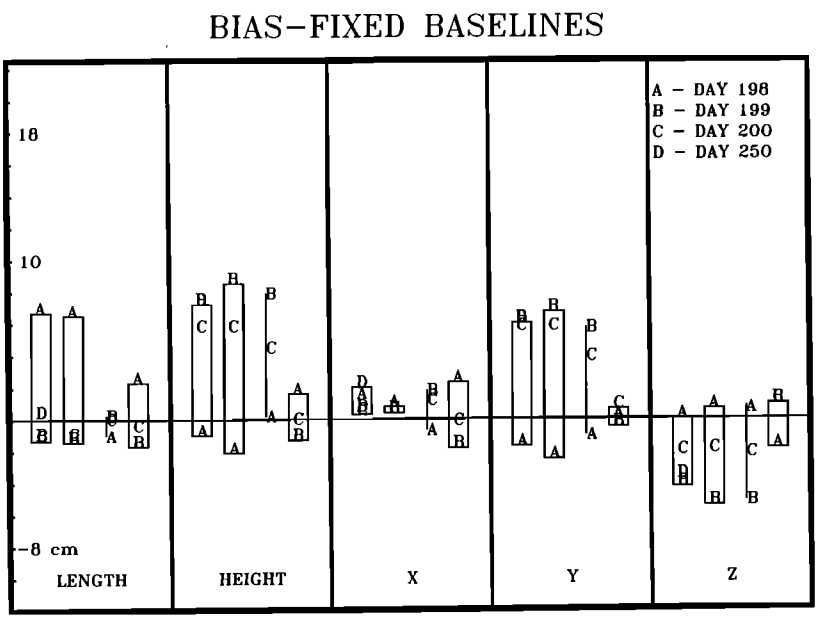

Fig. 4. Bias-fixed baseline solutions, normalized to the average of WVR corrected results (set S_{wvr}). Baseline length, height, and coordinate solutions are shown for the following three data sets, left to right: (1) T_{sm}, total receiver data set. This set uses default surface met values (P = 840 mbar, T = 25 ° C, RH = 50%) to correct for tropospheric path delay. (2) S_{sm}, receiver subset with simultaneous WVR data. This subset uses default surface met values to correct for tropospheric path delay. (3) S_{wvr}, receiver subset with simultaneous WVR data. This subset uses WVR and default P and T values to correct for tropospheric path delay. Simulated solutions for set S_{sm} that contain only the wet path delays estimated from WVR data are shown as vertical lines. WVR correction brings the simulated solutions for all 3 days into perfect agreement.

a factor of 3.7 (to 0.6 ppm). In the bias-free case (Table 3) the same 4-cm vertical decrease occurs, with repeatability improved by a factor of 1.9 (to 1 ppm). This decrease is confirmed by the simulated vertical solutions which are plotted in Figures 4 (bias-fixed) and 5 (bias-free). In the bias-fixed case where measured P and T values and either WVR data or measured RH values were used (Table 4), the vertical also decreases by 4 cm when the WVR correction is applied, and repeatability improves by a factor of 2.6 (to 0.6 ppm).

A comparison of Tables 2 and 4 shows an improvement in repeatability (for T_{sm} and S_{sm}) when we include the time varying values for P, T, and RH. In contrast, the WVR-corrected results (S_{wvr}) are not significantly affected by the interpolated P and T corrections. Thus the surface met corrections, compared to default corrections, improve the repeatability significantly (by a factor of 2.6 in length) when WVR corrections are not used. Therefore it is worthwhile to perform these measurements frequently and carefully. For example, surface met instruments should be shielded from sunlight and should be elevated to reduce surface effects.

Because of the short duration of the observations in 1983, it might be argued that the tropospheric errors would tend to average out for longer durations. We offer two comments regarding this argument. First, comparing the solutions in Table 2 for day 199, sets T_{sm} and S_{sm}, we find that they agree to 1.3 cm (vertical) or less. In spite of the fact that T_{sm} contains 224 points, compared to 113 points for S_{sm}, the solution was not significantly changed. However, a significant change does occur (4 cm in the vertical) when the WVR corrections are applied. Since this change is also seen in the simulations, the WVR correction is responsible rather than the 40% decrease in available data. Second, we find a similar change in the vertical results for day 200, when a more favorable duration and distribution of satellites was observed.

As seen in Tables 2-4, the vertical component from the 1984 measurement exceeds the WVR-corrected 1983 measurements by 8 cm. This is surprising because the weather conditions in 1984 were dry and clear. However, we note that a similar 8-cm decrease occurred with WVR correction for days 199 and 200 in 1983. It was only day 198 that was increased by the correction. The trend seen in Figure 2, where the Boulder wet path exceeds Erie except for day 198, confirms this behavior. If this same trend occurred on day 250 in 1984, it would account for this discrepancy. Of course, possible orbit and ionospheric errors cannot be disregarded. Consider the ratio of the precise ephemeris accuracy (30 m) to the orbit radius (25,000 km), which is an estimate of the effect of orbit error on baseline accuracy

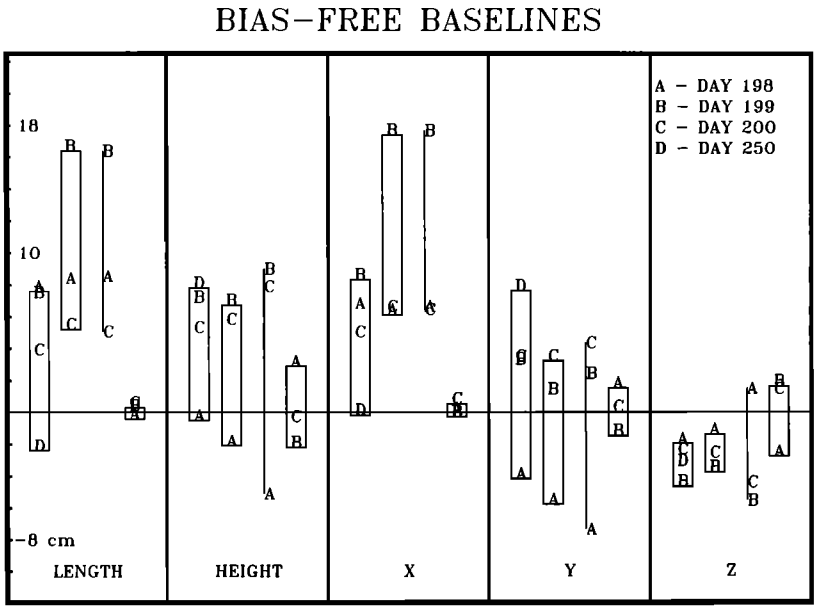

Fig. 5. Bias-free baseline solutions, normalized to the average of bias-free WVR corrected results (set S_{wvr}). Other features are described in the caption to Figure 4.

[Beutler et al., 1984]. Multiplying this ratio by the baseline length we estimate the influence of orbit error to be 1.2 ppm x 22 km = 2.6 cm. The ionospheric error for a similar 22-km baseline measured by dual-band receivers was found to be 1.0 cm for the L1 band [Crow et al., 1984]. However, the measurement was performed at night when the ionosphere is typically less active. According to Spilker [1978], the mean ionospheric daytime delay exceeds the mean nighttime delay by a factor of 3. We therefore estimate the ionospheric error for our daytime L1 measurements to be 3 cm. Assuming that the orbit and ionospheric errors are independent, they sum to 4 cm. Thus even though the satellite duration and distribution were favorable on day 250 and taking into account a reasonable estimate for orbit and ionospheric errors, a significant error in the vertical component occurred which might have been corrected if WVR data had been available.

There is a marked contrast in the repeatability of the surface met corrected east-west (approximately the X direction) components, comparing the bias-fixed and bias-free results in Figures 3 and 4. For bias-fixed solutions the geometric strength is a function of the distribution of satellite locations as viewed from the ground stations. For bias-free solutions the geometric strength depends upon the distribution of satellite velocities. Observing the current GPS constellation from mid-latitudes, the satellites are viewed in essentially all directions, but their velocities are principally north-south (see Figure 1). Hence the geometry for bias-fixed solutions is inherently stronger than for bias-free solutions. In addition, bias-free solutions are weakened by the fact that the biases must be treated as additional estimated parameters, thus diluting the geometric strength of the data in estimating baseline components.

WVR correction of wet path errors enhanced our ability to select the correct phase bias. This is not surprising, considering that the WVR corrections were as large as 10 cm, which is the same magnitude as the 9.5-cm effective carrier wavelength. For example, our success in meeting our bias-fixing criteria for all three days of data using WVR corrections, and the failure using surface met (or default) corrections represent this enhancement (see Tables 2 and 4). In fact, for set S_{sm}, day 199, the automatic bias-fixing solution disagreed by 12 cm in length with the listed value. As mentioned in the footnote to Tables 2 and 4, we forced the listed solution by selecting bias values determined for the set S_{wvr}, day 199. If this single measurement had been performed alone, with no WVR corrections available, this 5 ppm error would have remained uncorrected.

In summary, we have seen that WVR or surface met corrections can significantly improve GPS baseline determinations. Therefore it seems highly desirable to obtain accurate and frequent WVR, P, and T data. We recognize that our limited data do not provide the statistical strength necessary to reach firm conclusions regarding the effect of tropospheric corrections on GPS baseline solutions. However, using the available data, we were able to look at the tropospheric signature and to roughly measure its influence on baseline components. We found that WVRs detected variations as large as 10 cm in the wet path delay. Corrections based on WVR data caused a decrease in the vertical baseline component by 4 cm and a corresponding improvement in repeatability by a factor of 3 to 0.6 ppm. The other components were affected by smaller amounts. We also found that WVR correction enhanced our ability to perform reliable bias fixing.

These findings suggest that WVR (and surface P and T) corrections may serve an important role in obtaining the high accuracy associated with bias-fixed solutions for baselines ranging from tens to perhaps hundreds of kilometers.

Acknowledgments. The authors thank David C. Hogg and John D. Bossler for their assistance in obtaining radiometers and receivers for this experiment; Clyde Goad for spline interpolation of the WVR data; Clyde Goad, Ben Remondi, Judah Levine, and Peter Bender for assistance in analysis; Roger Bilham, Richard Cohen, Larry Slater, and Max Wyss for assistance in pointing WVRs; Jack Snider for the collection and analysis of WVR data; Claudia Rogers-Anderson for assistance in preparation of tables and figures; the Bureau of Reclamation and the NOAA for the use of their WVRs; the NGS for acquisition and assistance in analysis of GPS data; the U.S. Geological Survey for financial support under grant 14-08-000121378; and the National Science Foundation for support under grant EAR8408005.

References

Bender, P. L., and D. R. Larden, GPS carrier phase ambiguity resolution over long baselines, paper presented at the First International Symposium on Precise Positioning with GPS, NOAA, Rockville, Md., 1985.

Beutler, G., D. A. Davidson, R. B. Langley, R. Santerre, P. Vanicek, and D. E. Wells, Some theoretical and practical aspects of geodetic positioning using carrier phase difference observations of GPS satellites, Surv. Eng., Tech. Rep. 109, Univ. of New Brunswick, Fredericton, 1984.

Bock, Y., R. I. Abbot, C. C. Counselman III, S. A. Gourevitch, and R. W. King, Establishment of three-dimensional geodetic control via interferometry with the Global Positioning System, J. Geophys. Res., 90, 7689-7703, 1985.

Bossler, J. D., C. C. Goad, and P. L. Bender, Using the Global Positioning System (GPS) for geodetic surveying, Bull. Geod., 54, 553-563, 1980.

Counselman, C. C., and D. H. Steinbrecher, The Macrometer: A compact radio interferometry terminal for geodesy with GPS, in Proceedings of the Third International Geodetic Symposium on Satellite Doppler Positioning, Vol. 2, pp. 1165-1172, Physical Sciences Lab, New Mexico State University, 1982.

Crow, R. B., F. R. Bletzacker, R. J. Najarian, G. H. Purcell, J. I. Statman, and J. B. Thomas, Series-X final engineering report, Rep. D-1476, Jet Propul. Lab., Pasadena, Calif., 1984.

Goad, C. C., Wallops Island tropospheric refraction study and analysis, prepared for H. R. Stanley Geos-C Project Scientist NASA/Wallops Station contract NAS 6-2173, 1974.

Goad, C. C., and B. W. Remondi, Initial relative positioning results using the Global Positioning System, Bull. Geod., 58, 193-210, 1984.

Hodgman, C. D., R. C. Weast, and S. M. Selby, Handbook of Chemistry and Physics, 42nd ed., pp. 2496-2497, Chemical Rubber, Cleveland, Ohio, 1961.

Hogg, D. C., F. O. Guiraud and M. T. Decker, Measurement of excess radio transmission length on earth-space paths, Astron. Astrophys., 95, 304-307, 1981.

Hogg, D. C., F. O. Guiraud, J. B. Snider, M. T. Decker, and E. R. Westwater, A steerable dual-channel microwave radiometer for measurement of water vapor in the troposphere, J. App. Meteorol., 22, 789-806, 1983.

Hopfield, H. S., Two-quartic tropospheric refractivity profile for correcting satellite data, J. Geophys. Res., 74, 4487-4499, 1969.

Remondi, B. W., Using the Global Positioning System (GPS) phase observable for relative geodesy: Modeling, processing, and results, Ph.D. thesis, Univ. of Tex. at Austin, Austin, 1984.

Saastamoinen, J., Contributions to the theory of atmospheric refraction, Bull. Geod., 105, 279-298, 1972a.

Saastamoinen, J., Contributions to the theory of atmospheric refraction, Bull. Geod., 106, 383-397, 1972b.

Saastamoinen, J., Contributions to the theory of atmospheric refraction, Bull. Geod., 107, 13-34, 1972c.

Spilker, J., GPS signal structure and performance characteristics, Navigation, 25, 121-146, 1978.

Strange, W. E., High precision three dimensional differential positioning using GPS, paper presented at the First International Symposium on Precise Positioning with GPS, NOAA, Rockville, Md., 1985.

Ware, R. H., C. Rocken, and J. B. Snider, Experimental verification of improved GPS-measured baseline repeatability using water vapor radiometer corrections, IEEE Trans. Geosci. Remote Sens., GE-23, 467-473, 1985.

K. J. Hurst, Lamont-Doherty Geological Observatory, Palisades, NY 10964

C. Rocken and R. H. Ware, CIRES, Box 449, University of Colorado, Boulder, CO 80309

(Received June 24, 1985;
revised January 28, 1986;
accepted February 14, 1986.)